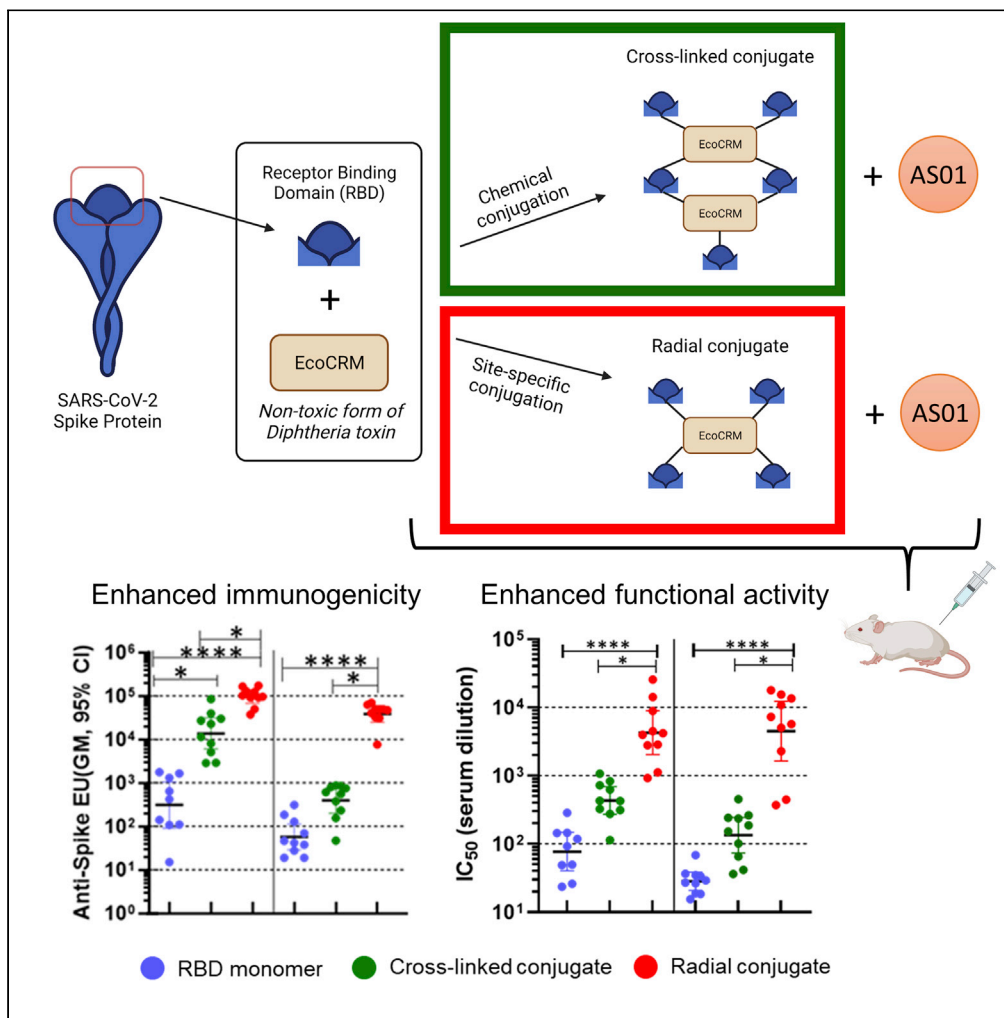**Article**

Protein-protein conjugation enhances the immunogenicity of SARS-CoV-2 receptor-binding domain (RBD) vaccines

Puthupparampil V. Scaria, Chris G. Rowe, Beth B. Chen, ..., Kelly M. Rausch, Niraj H. Tolia, Patrick E. Duffy

patrick.duffy@nih.gov

Highlights

Conjugation of RBD to EcoCRM enhanced its immunogenicity in the mouse study

Radial conjugate of RBD in AS01 induced strong pseudovirus neutralization activity

RBD conjugates induced Th-1 response with AS01 and Th-2 response with Alhydrogel

Article

Protein-protein conjugation enhances the immunogenicity of SARS-CoV-2 receptor-binding domain (RBD) vaccines

Puthupparampil V. Scaria,[1] Chris G. Rowe,[1] Beth B. Chen,[1] Thayne H. Dickey,[1] Jonathan P. Renn,[1] Lynn E. Lambert,[1] Emma K. Barnafo,[1] Kelly M. Rausch,[1] Niraj H. Tolia,[1] and Patrick E. Duffy[1,2,*]

SUMMARY

Several effective SARS-CoV-2 vaccines have been developed using different technologies. Although these vaccines target the isolates collected early in the pandemic, many have protected against serious illness from newer variants. Nevertheless, efficacy has diminished against successive variants and the need for effective and affordable vaccines persists especially in the developing world. Here, we adapted our protein-protein conjugate vaccine technology to generate a vaccine based on receptor-binding domain (RBD) antigen. RBD was conjugated to a carrier protein, EcoCRM®, to generate two types of conjugates: crosslinked and radial conjugates. In the crosslinked conjugate, antigen and carrier are chemically crosslinked; in the radial conjugate, the antigen is conjugated to the carrier by site-specific conjugation. With AS01 adjuvant, both conjugates showed enhanced immunogenicity in mice compared to RBD, with a Th1 bias. In hACE2 binding inhibition and pseudovirus neutralization assays, sera from mice vaccinated with the radial conjugate demonstrated strong functional activity.

INTRODUCTION

The COVID-19 agent SARS-CoV-2 emerged in late 2019 and has since caused over 332 million infections and 5.5 million deaths worldwide as of Jan. 19, 2022 (https://covid19.who.int). The pandemic has spurred unprecedented efforts to develop vaccines that contain virus spread or prevent disease, resulting in numerous effective products as well as vaccine candidates based on proven technologies, such as inactivated viral particles as well as emerging technologies including mRNA and adenoviral platforms (Bok et al., 2021; Baden et al., 2021; Voysey et al., 2021; Polack et al., 2020; Sadoff et al., 2021; Alderson et al., 2021; Hasegawa, 2021; Hotez and Bottazi, 2022). mRNA and viral vector platforms were under development for various vaccines and benefitted from the resources and sense of urgency brought on by the pandemic to rapidly generate highly effective vaccines against SARS-CoV-2 (Mendonça et al., 2021; Armbruster et al., 2019; Sebastian et al., 2019; Richner et al., 2017; Pardi et al., 2020; Petsch et al., 2012; Collignon et al., 2020). Despite these historic successes, SARS-CoV-2 continues to surge across the world, generating variants that threaten the effectiveness of existing vaccines (Tao et al., 2021). Thus, new candidates and new vaccine technologies that can be scaled up rapidly remain a research priority to address the ongoing COVID-19 threat as well as threats from new pathogens or variants that may appear in future (Heath et al., 2021; Ndwandwe and Wiysonge, 2021; Maharjan and Choe, 2021).

In addition to the vaccine platform, the identification of the optimal target or targets is critical to vaccine success. The design of vaccines against SARS-CoV-2 relied on earlier work that identified the Spike protein as the key target in the coronavirus agents of SARS-CoV and MERS (Martin et al., 2008; Du et al., 2009; Kirchdoerfer et al., 2016; Pallesen et al., 2017). Vaccines against the Spike protein, which is used by SARS-CoV-2 to bind the human ACE2 receptor and enter host cells, have shown efficacy using different platforms albeit at varying levels (Jackson et al., 2022).

The SARS-CoV-2 Spike protein is a large protein (141 kDa) that generates numerous antibodies against various epitopes within the protein (Voss et al., 2021). Neutralizing antibodies that block SARS-CoV-2 binding to ACE2 and entry into human cells primarily bind epitopes in the receptor-binding domain (RBD) of the Spike protein (Xiaojie et al., 2020). Thus, RBD is an attractive antigen to focus the immune response and

[1]Laboratory of Malaria Immunology and Vaccinology, NIAID/NIH, 29 Lincoln Drive, Building 29B, Bethesda, MD 20892-2903, USA

[2]Lead contact

*Correspondence: patrick.duffy@nih.gov

https://doi.org/10.1016/j.isci.2022.104739

Table 1. Amino acid sequence and physico-chemical characteristics of immunogens

Conjugate	Lot #	Ave. mol. wt (kDa)[a]	Mol. wt range (kDa)[a]	Conj. Composition[b]	Comments
RBD-EcoCRM-RC	MV-8195	220	214–245	63%(w/w)Ag; 3.8 Ag/Carrier	Radial conjugate
RBD-EcoCRM-CC	MV-8198	1,364	613–3,163	49%(w/w)Ag; 2.2 Ag/carrier	Crosslinked conjugate
RBD	NA	31.5	NA	NA	Monomer
EcoCRM®	NA	58.4	NA	NA	Monomer

(A) Amino acid sequence (AA_{319} to AA_{541}) of the receptor-binding domain of the wild-type SARS-CoV-2 virus spike protein used in this study with a C-terminal His Tag.

(B) Physico-chemical characteristics of crosslinked conjugate (RBD-EcoCRM-CC) and radial conjugate (RBD-EcoCRM-RC) of RBD with EcoCRM®. Average molecular weight and molecular weight distribution were determined by SEC-MALS analyses and conjugate compositions were determined by amino acid analysis.

RBD sequence (9C)

RVQPTESIVRFPNITNLCPFGEVFNATRFASVYAWNRKRISNCVADYSVLYNSASFSTFKCYGVSPTKLNDLCFTNVYADSFVIRGDEVRQIAPGQTGKIADYNYKLPDDFTG CVIAWNSNNLDSKVGGNYNYLYRLFRKSNLKPFERDISTEIYQAGSTPCNGVEGFNCYFPLQSYGFQPTNGVGYQPYRVVVLSFELLHAPATVCGPKKSTNLVKNKCVNFH HHHHH.

[a]Molecular weight & molecular weight distribution of conjugate were determined by SEC-MALS analysis.

[b]Conjugate compositions were determined by amino acid analysis.

maximize the generation of neutralizing antibodies (Kleanthous et al., 2021). Efforts to develop RBD-based vaccines have resulted in two successful vaccines, a Tetanus Toxoid conjugate of RBD with Alum adjuvant (Soberana 02) and RBD adjuvanted with Alum and CpG 1018 (Corbevax™), currently approved for human use in Cuba and India, respectively (Toledo-Romani et al., 2021; Nanishi et al., 2021; Valdes-Balbin et al., 2021). Strategies to enhance the immunogenicity of RBD involve the structural optimization of the antigen and/or presentation of the antigen in particulate, multimeric formats such as nanoparticles or virus-like particles (VLPs) (Dickey et al., 2021; Hsieh et al., 2020; Nguyen and Tolia, 2021; Walls et al., 2020; Saunders et al., 2021; Gaspar et al., 2021; Tan et al., 2021; Geng et al., 2021; Volpatti et al., 2021; Wong et al., 2022).

We have previously developed a protein-protein conjugate nanoparticle technology to enhance the immunogenicity of poorly immunogenic malaria antigens, wherein the target antigen is chemically conjugated to a carrier protein forming crosslinked nanoparticles (Shimp et al., 2013; Jones et al., 2016; Scaria et al., 2017). The effectiveness of this technology has been evaluated in several preclinical and clinical studies (Scaria et al., 2019, 2020, 2021; Talaat et al., 2016; Sagara et al., 2018; Healy et al., 2021). Phase II clinical evaluation of a malaria transmission-blocking vaccine that was manufactured using this technology is currently underway in Mali (Clinical Trials Identifier: NCT03917654). Here, we adapted this vaccine technology to generate an RBD-based vaccine for SARS-CoV-2. RBD was conjugated to the carrier protein EcoCRM®, a version of CRM197 (the non-toxic mutant of diphtheria toxin) expressed in *E. coli* and developed for clinical use by Fina Biosolutions LLC. Conjugation to EcoCRM® has been shown to enhance the immunogenicity of malaria antigens (Scaria et al., 2020).

Here, two different types of conjugates were synthesized, formulated with clinical adjuvants Alhydrogel® or AS01, and evaluated in mouse immunogenicity studies. Conjugation and formulation in AS01 significantly enhanced RBD conjugate vaccine immunogenicity and functional activity, demonstrating the potential for this approach to generate vaccine candidates against SARS-CoV-2.

RESULTS

Synthesis and characterization of conjugate vaccines

The receptor-binding domain (RBD) used in this study corresponds to AA_{319} through AA_{541} of Spike protein from the parent SARS-CoV-2 (WA-1) variant (Table 1A), with two N-glycosylation sites at N_{331} and N_{343}. The recombinant antigen expressed in mammalian cells yielded a molecular weight of 31.5 kDa by SEC-MALS analysis as opposed to expected 25,098 based on the protein sequence, suggesting that one or both sites are glycosylated. The RBD antigen also has an unpaired cysteine near its carboxyl-terminus that can be used for conjugation. The unpaired cysteine side chain was capped with a Glutathione during expression, preventing significant dimerization of the protein. The protecting Glutathione was easily removed by five molar equivalents (mEq) of DTT without reducing the disulfide bonds, thus enabling site-specific conjugation with the sulfhydryl group of unpaired cysteines.
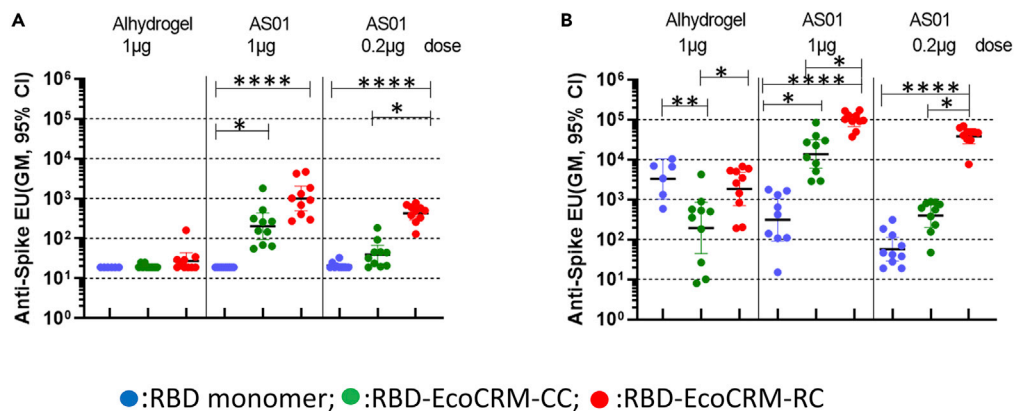
Figure 1. Immunogenicity of RBD and RBD conjugates formulated with Alhydrogel® or AS01

Comparison of serum anti-spike antibody levels in mouse sera following vaccination with RBD, RBD-EcoCRM-CC, and RBD-EcoCRM-RC formulated with Alhydrogel or AS01, measured on day 14 (A) and on day 35 (B). Mice (n = 10) were vaccinated on day 0 and day 21 by intramuscular injection with 1 ug dose of RBD in Alhydrogel or 1 ug or 0.2 ug dose of RBD formulated with AS01. For conjugates, the dose corresponds to the among of RBD in the conjugates. Sera from each animal were analyzed by ELISA in triplicate and the y-axis represents the geometric mean of ELISA units with a 95% confidence interval. Statistical differences between groups were measured using a Kruskal-Wallis one-way ANOVA followed by a Dunn multiple comparator test. *p ≤ 0.05, **p ≤ 0.01, ***p ≤ 0.001, ****p ≤ 0.0001.

The two different types of antigen-carrier conjugates, referred to as "crosslinked conjugates (CC)" and "radial conjugates (RC)," were synthesized by chemically conjugating RBD to the EcoCRM® carrier protein (Figures S1A and S1B). For the crosslinked conjugate, antigen and carrier proteins are chemically cross-linked at multiple sites to form nanoparticles using our protein-protein conjugation method (Jones et al., 2016; Scaria et al., 2017, 2019). This method employs the lysine sidechains of antigen and carrier to enable crosslinking. For the radial conjugate, RBD antigen was conjugated to maleimide modified EcoCRM® through its unpaired cysteine sidechain. (Figure S1).

Physico-chemical characteristics of the conjugates including the molecular weight and composition are given in Table 1B. The weighted average molecular weight of the conjugates was determined by SEC-MALS analysis (Figures S2A and S2B) and conjugate composition (antigen-to-carrier) was analyzed by an amino acid analysis method routinely used for various protein-protein conjugates in our laboratory (Scaria et al., 2020). The radial conjugate (RBD-EcoCRM-RC) had a weighted average molecular weight of 220 kDa with a molecular weight distribution ranging between 214 kDa and 245 kDa. This conjugate had a mass composition of 63% (w/w) antigen and 37% carrier which corresponds to an approximately 3.8 molar ratio of antigen to carrier. The crosslinked conjugate (RBD-EcoCRM-CC) was larger with a weighted average molecular weight of 1,364 kDa and distribution of 623–3,163 kDa. This conjugate had a composition of 49% antigen content which corresponds to ∼2.2 molar ratio of antigen to carrier. Both RBD-EcoCRM-RC and RBD-EcoCRM-CC show a smeared pattern on an SDS gel, indicative of the molecular weight distribution (Figure S3A). Both conjugates were able to bind an RBD-specific monoclonal antibody (CR3022) by Western blot, indicating that the chemical modifications did not abolish antibody binding (Figure S3B).

Immunogenicity in mice

RBD-EcoCRM-RC and RBD-EcoCRM-CC along with unconjugated monomer RBD were evaluated in mouse studies to assess immunogenicity and serum functional activity. RBD monomer, as well as the two conjugates, were formulated with Alhydrogel® or AS01, two adjuvants currently used in approved human vaccines (Nanishi et al., 2020).

Levels of serum IgG antibodies that recognize full-length Spike protein were measured by ELISA. On day 14, two weeks after the first vaccination, monomer, as well as RBD-EcoCRM-CC conjugate formulated in Alhydrogel®, yielded no measurable antibody response against Spike protein (Figure 1A). An antibody response above the background level appeared in a few animals that received RBD-EcoCRM-RC formulated in Alhydrogel®.
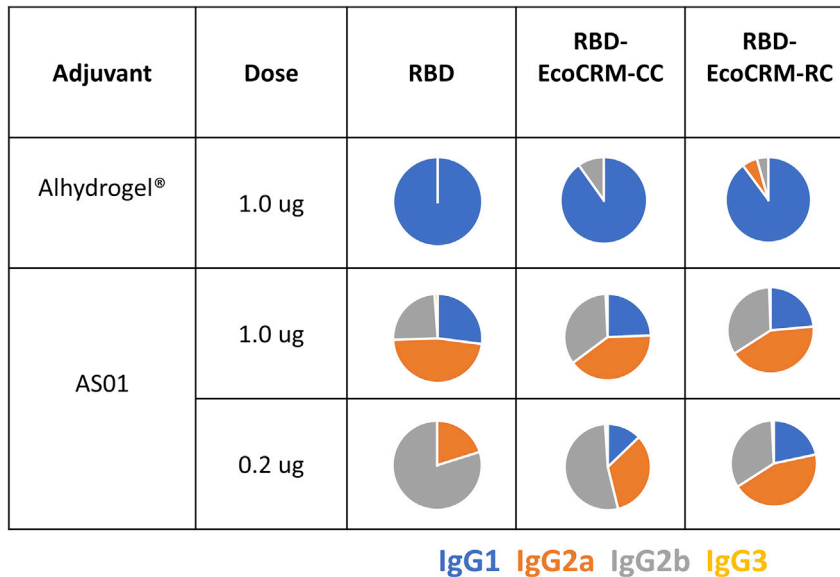
Adjuvant	Dose	RBD	RBD-EcoCRM-CC	RBD-EcoCRM-RC
Alhydrogel®	1.0 ug			
AS01	1.0 ug			
	0.2 ug			

IgG1 IgG2a IgG2b IgG3

Figure 2. IgG subclass distribution in the immune sera

IgG subclass (IgG1, IgG2a, IgG2b, and IgG3) distribution of sera from mice vaccinated with RBD and its conjugates, RBD-EcoCRM-CC and RBD-EcoCRM-RC, formulated with Alhydrogel or AS01. Immune sera collected on day 35 after two vaccinations (days 0 and 21) were analyzed by ELISA using pooled samples for each group using isotype-specific goat-anti-mouse secondary antibodies from Southern Biotech, Birmingham AL.

When formulated in AS01, on the other hand, both conjugates gave significantly higher levels of antibody response compared to the monomer RBD. At the 1.0 µg dose, antibody levels did not differ significantly between the two conjugates on day 14, albeit RBD-EcoCRM-RC antibody responses trended higher. At the 0.2 µg dose, a similar pattern in antibody levels was observed, but in this case, RBD-EcoCRM-RC antibody responses were significantly higher than those in RBD-EcoCRM-CC conjugate as well as monomeric RBD groups.

Antibody levels measured two weeks after the second vaccination showed substantial increases for all groups (Figure 1B). In Alhydrogel®, RBD-EcoCRM-CC had significantly lower levels of antibody compared to monomer and RBD-EcoCRM-RC; monomer was not significantly different from RBD-EcoCRM-RC in antibody responses. In AS01, both conjugates achieved significantly higher antibody responses than the monomer, and the response to RBD-EcoCRM-RC was significantly higher than those to RBD-EcoCRM-CC. At 1.0 µg dose in AS01, the antibody level of the RBD-EcoCRM-RC group was >300-fold higher than that of the monomer group (GM 96,442 vs 309 ELISA units). At 0.2 µg dose, RBD-EcoCRM-RC antibody response was 680- and 97-fold higher than those of monomeric RBD and RBD-EcoCRM-CC, respectively. Antibody levels of RBD-EcoCRM-RC at 0.2 µg and 1.0 µg doses did not differ significantly.

When comparing the effect of the two adjuvants, both conjugates gave significantly higher antibody levels in AS01 compared to Alhydrogel® on Day 35 at 1.0 ug doses (p = 0.0074, RBD-EcoCRM-CC, Alhydrogel® vs AS01; p = 0.0007, RBD-EcoCRM-RC, Alhydrogel® vs AS01). At 1.0 µg dose, the geometric mean antibody level of RBD-EcoCRM-RC in AS01 was 52-fold higher than that of RBD-EcoCRM-RC in Alhydrogel®, while the levels of antibody for RBD-EcoCRM-CC in AS01 was 70-fold higher than those for this conjugate in Alhydrogel®. In AS01, RBD-EcoCRM-RC gave significantly higher antibody levels than RBD-EcoCRM-CC at both 1.0 and 0.2 µg doses.

IgG subclass distribution

IgG subclass (IgG1, IgG2a, IgG2b, and IgG3) distribution in immune sera from vaccinated mice was analyzed by ELISA using the secondary antibody specific to each subclass. Alhydrogel® formulated RBD, both as monomer and conjugates, showed an IgG1 dominant subclass distribution with very low levels of IgG2, indicating a strong Th2 polarized immune response (Figure 2). The IgG response to RBD monomer was almost exclusively IgG1, while that to the conjugate was largely IgG1 with modest IgG2
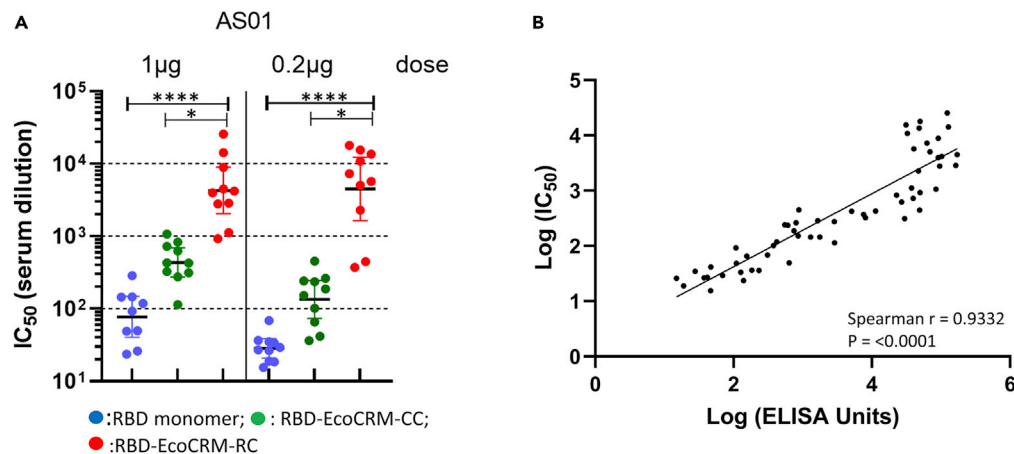
hACE2 Binding Inhibition

Figure 3. Immune sera block the binding of ACE2 to RBD

Effect of immune sera on the binding of hACE2 to RBD was assayed by ELISA and the binding inhibitory activity of sera is presented as IC_{50}, the serum dilution at which the binding inhibitory activity is reduced by 50%.

(A) Comparison of the binding inhibitory activity of sera from mice vaccinated with AS01 formulated RBD and its conjugates with 1 ug or 0.2 ug dose of RBD. Error bars represent geometric mean with 95% confidence limit.

(B) Plot of Log (ELISA units) vs Log (IC_{50}) showing a strong correlation (Spearman r = 0.9332; p = <0.0001) between the serum antibody levels and binding inhibitory activity. Statistical differences between groups were measured using a Kruskal-Wallis one-way ANOVA followed by a Dunn multiple comparator test. *p ≤ 0.05, **p ≤ 0.01, ***p ≤ 0.001, ****p ≤ 0.0001.

contribution. On the other hand, sera from mice vaccinated with AS01-formulated immunogens showed a qualitatively different IgG subclass distribution with a greater contribution of IgG2 relative to IgG1. AS01-formulated antigens primarily comprised IgG2a and/or IgG2b, with modest or no IgG1, indicating a mixed Th1/Th2 response with a dominant Th1 polarization.

Human ACE2 (hACE2) binding inhibition by immune sera

The functional activity of immune sera was analyzed by measuring its ability to block the binding of RBD to its hACE2 receptor. RBD was immobilized on a plate and tagged hACE2 binding was measured by ELISA. Binding was measured in the presence of serially diluted serum and the IC_{50} (serum dilution that gave a 50% reduction in Spike binding to hACE2) was determined for each animal (Figure 3A). Only the sera from animals that received AS01-formulated immunogens were analyzed as the immunogenicity of Alhydrogel® formulated antigens was significantly lower.

Sera from mice vaccinated with either of the two conjugates or the monomer inhibited the binding of Spike protein to the hACE2 receptor. The binding inhibition activity of the three immunogens corresponded to their antibody levels. RBD-EcoCRM-RC showed significantly higher binding inhibition activity (higher IC_{50}) than the monomer and RBD-EcoCRM-CC at both 1.0 μg and 0.2 μg doses (Figure 3A). For both doses, RBD-EcoCRM-RC serum was significantly more effective than RBD-EcoCRM-CC serum in blocking Spike-receptor binding. hACE2 binding inhibitory antibody levels of RBD-EcoCRM-RC animals were 55 and 159-fold higher than those of the monomer animals at 1.0 μg and 0.2 μg doses, respectively. As with serum antibody levels, RBD-EcoCRM-RC did not yield significantly different inhibitory antibody levels at the two doses. A plot of serum ELISA unit vs IC_{50} shows a strong correlation between the serum antibody level and hACE2 binding inhibitory antibody level (Spearmen r = 0.9332; p = <0.0001) (Figure 3B).

Pseudovirus neutralization assay

Immune sera were tested for virus neutralization activity using a pseudovirus with wild-type (WA-1) SARS-CoV-2 spike protein-expressing luciferase reporter gene. Only the sera from animals vaccinated with immunogens formulated with AS01 were tested and sera for each group were pooled for these analyses. Figure 4A shows the percentage inhibition of pseudovirus entry into HEK293 cells overexpressing ACE2 at
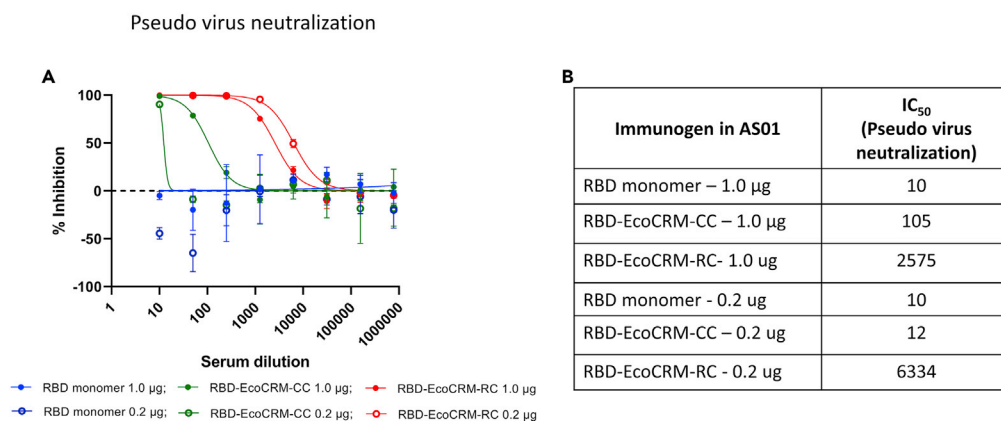
Pseudo virus neutralization

A

B

Immunogen in AS01	IC_{50} (Pseudo virus neutralization)
RBD monomer – 1.0 µg	10
RBD-EcoCRM-CC – 1.0 µg	105
RBD-EcoCRM-RC- 1.0 ug	2575
RBD monomer - 0.2 ug	10
RBD-EcoCRM-CC – 0.2 ug	12
RBD-EcoCRM-RC - 0.2 ug	6334

Figure 4. Pseudovirus neutralization

(A) Effect of immune sera on the internalization of a pseudovirus with WA-1 SARS-CoV-2 virus spike protein, expressing luciferase gene into human ACE2 expressing HEK293 cells. Binding curves were generated by assaying virus internalization (by luciferase gene expression) in the presence of different dilutions of immune sera. Pooled sera for each group were used for this analysis. IC_{50}, defined as the serum dilution that reduced the pseudoviral uptake by 50%, was calculated from the biding curve. Each point represents the mean of triplicate measurement and error bars represent standard error of the mean.

(B) IC_{50} values determined for sera from mice vaccinated with RBD and its conjugates (1.0 ug and 0.2 ug doses) formulated with AS01.

different dilutions of mice sera. IC_{50} values, defined as the dilution that gives 50% inhibition of pseudovirus entry, are listed in the table (Figure 4B). Sera from mice vaccinated with RBD monomer at either dosage were unable to block viral entry. Similarly, sera from RBD-EcoCRM-CC also were poor inhibitors of viral entry, although 1.0 µg dose gave a measurable IC_{50} of 105. In contrast, sera from mice immunized with RBD-EcoCRM-RC conjugate showed strong virus neutralization activity. Groups that received 1.0 µg dose, as well as 0.2 µg dose, showed this strong activity, albeit the low dose group achieved a higher IC_{50} than the high dose group (IC_{50} 6334 and 2575 for low and high dose groups, respectively).

DISCUSSION

Chemical conjugation of bacterial polysaccharides to protein carriers has generated effective vaccines against bacterial infections (Pichichero, 2013). In a similar strategy, we have developed a protein-protein conjugate vaccine platform for malaria antigens and demonstrated its manufacturability and effectiveness in clinical trials (Shimp et al., 2013; Talaat et al., 2016; Sagara et al., 2018; Healy et al., 2021). Here, we adapted this technology for a prototype vaccine against SARS-CoV-2 using its receptor-binding domain (RBD) as the antigen. Using RBD as an immunogen has the advantage of focusing the antibody response on the domain that binds to the receptor and facilitates viral entry into human cells. Most currently approved vaccines target the full-length Spike protein or the whole virus. In addition to neutralizing antibodies, these approaches have the potential to generate non-neutralizing antibodies against different epitopes of the virus and can contribute to antibody-dependent enhancement of infection or disease (Kleanthous et al., 2021). Thus, strategies to minimize these possibilities while directing the antibody response to the binding site may be advantageous.

While RBD monomer in Alhydrogel® was moderately immunogenic (GM EU 3284), RBD monomer yielded a weaker antibody response in AS01 (GM EU 309). In Alhydrogel®, RBD monomer gave a similar or higher antibody titer compared to radial and crosslinked conjugates, respectively. In contrast, both crosslinked and radial conjugates showed high antibody responses in AS01: antibody levels at the 1.0 µg dose were 4.2 and 29.4-fold higher compared to RBD in Alhydrogel® for cross-linked and radial conjugates, respectively.

Synthesis of crosslinked conjugate involves random modification of lysine sidechains in the antigen to allow crosslinking with carrier protein. This process has the potential to also modify lysine residues in epitopes critical for the generation of functional antibodies and this might affect the overall functional activity of immune sera. The radial conjugate on the other hand is generated by site-specific conjugation through a

cysteine side chain without the chemical modification of any other residues in the antigen. This unmodified antigen conjugated to the carrier appears to provide a superior functional activity.

As the immune response with Alhydrogel® was relatively modest for the conjugates, studies of functional activity only focused on AS01-formulated RBD monomer and conjugates. The human ACE2 binding inhibition assay showed efficient blocking of RBD/ACE2 binding interaction by the immune sera from mice vaccinated with the two conjugates. Nevertheless, the radial conjugate showed a significantly stronger binding inhibition activity compared to the crosslinked conjugate, both at 1.0 μg as well as 0.2 μg dose. This activity correlated strongly with the total antibody levels. Pseudovirus neutralization assay further demonstrated the superior functional activity of the radial conjugate in blocking the ACE2-mediated virus uptake by ACE2-expressing cells. Interestingly, the low dose radial conjugate gave the highest pseudovirus neutralization titer. Pseudovirus used in this assay had the Spike protein from the wild-type SARS2-CoV-2. The effect of the immune sera on different variants has not been studied. Vaccines currently in use also target the wild-type Spike protein and they all appear to be effective against different variants when serum neutralizing antibody levels are sufficiently high (Barda et al., 2021). Furthermore, replacing the wild-type RBD with a variant RBD is feasible and straightforward if necessary.

Although a direct comparison of results from different laboratories is difficult to make, it is interesting to note that our radial conjugate-induced hACE2 receptor-binding inhibition activity and pseudovirus neutralization activity that match or exceed the activity of some of the currently approved vaccines when tested in mice (Valdes-Balbin et al., 2021; Corbett et al., 2020; Tian et al., 2021). Sera from mice vaccinated with 1.0 μg of mRNA-1273 (Moderna) yielded pseudovirus neutralization activity (IC_{50}) in the range of 89 to 1,115 in 3 different mouse strains [Figure 2 in 52], whereas mice vaccinated twice with RBD-EcoCRM-RC conjugate at 0.2 μg dose yielded an IC_{50} of 6,334 (Figure 4). Similarly, receptor blocking activity of immune sera from mice immunized twice with a vaccine based on full-length spike protein on a nanoparticle platform (NVX-CoV2373; Novavax) in the dose range of 0.05 to 10 μg yielded a receptor blocking activity with IC_{50} of 218–1642 (Tian et al., 2021), compared to IC_{50} of 7,882 obtained for mouse sera from RBD-EcoCRM-RC vaccinated mice (Figure 4). An RBD- Tetanus Toxoid conjugate vaccine with an efficacy >70% against Beta and Delta variants, approved for human use in Cuba (Finlay Vaccine Institute, Havana, Cuba), yielded ACE2 receptor blocking and virus neutralization activity with IC_{50} values of approximately 2,500 in mice (Toledo-Romani et al., 2021; Valdes-Balbin et al., 2021). Functional activity of RBD-EcoCRM-RC conjugate observed in this study clearly shows its potential to be an effective vaccine and further studies to explore this potential are warranted.

The adjuvants used in this study, Alhydrogel® and AS01, are both used in currently approved human vaccines (Lee and Nguyen, 2015; Garçon and Di Pasquale, 2017). Alhydrogel® is known to induce a Th2-biased immune response with protein subunit antigens (Scaria et al., 2020). This study showed a similar pattern: Alhydrogel® induced a Th2-skewed response dominated by IgG1 subclass against both monomer as well as conjugated RBD. AS01, which incorporates two immune potentiators (the TLR4 agonist MPL and the saponin QS-21), gave a mixed IgG subclass distribution with larger contributions from IgG2a and IgG2b compared to IgG1, indicating a Th1-biased immune response (Coccia et al., 2017). A mixed immune response inducing multiple antibody subclasses may be beneficial for an effective antiviral activity involving receptor-binding inhibition as well as other antibody-mediated effector functions such as complement-dependent cytotoxicity (CDC), antibody-dependent cellular cytotoxicity (ADCC), and antibody-dependent cellular phagocytosis (ADCP) (Natarajan et al., 2020; Tay et al., 2019).

While highly effective vaccines employing novel technologies such as mRNA are widely available in the US and other developed countries, neither these vaccines nor the underlying vaccine technologies are easily accessible to most of the developing world. This limits our ability to control the spread of the virus on a global scale and may lead to the generation of new variants in under-vaccinated and unvaccinated population, extending the pandemic. Developing vaccine technologies more readily available to other parts of the world for manufacturing and distribution is critical to bringing the pandemic under control as well as stopping the generation of new variants. Protein conjugation technology can be transferred relatively easily to vaccine manufacturers in developing countries for cost-effective vaccine manufacturing and distribution.

Limitations of the study

The present study focused on enhancing the immunogenicity of RBD antigen by chemical conjugation to a carrier protein, EcoCRM®. This was carried out in CD-1 mice and the sera were analyzed for the inhibition of

receptor binding and neutralizing antibody titers. Whether the level of antibody generated by the animals is sufficient for protection from live viral challenge could not be assessed in these animals. Future studies should be performed in hACE2-expressing mouse models to analyze the protective efficacy of this vaccine candidate. In addition, this study only compared the conjugate to the unconjugated RBD, and not to any other vaccines currently approved for human use. Although neutralizing antibody titers observed for the radial conjugate are comparable to or better than published results for some approved COVID-19 vaccines (when tested in mice), no direct comparison was made in the animal study. Future studies should assess this vaccine candidate in nonhuman primate models with currently approved vaccines as comparators, to establish the potential of this vaccine candidate.

STAR★METHODS

Detailed methods are provided in the online version of this paper and include the following:

- KEY RESOURCES TABLE
- RESOURCE AVAILABILITY
  - Lead contact
  - Materials availability
  - Data and code availability
- EXPERIMENTAL MODEL AND SUBJECT DETAILS
  - Mouse immunogenicity study
- METHOD DETAILS
  - Expression of full-length spike protein and receptor binding domain of SARS-CoV-2
  - Ace2-Fc expression and purification
  - Adjuvants
  - Chemicals and reagents
  - Maleimide modified EcoCRM
  - Sulfhydryl modified RBD
  - Synthesis of RBD-EcoCRM crosslinked conjugate (CC)
  - Synthesis of RBD-EcoCRM radial conjugate (RC)
  - Determination of thiol and maleimide modifications
  - Determination of conjugate molecular weight
  - Determination of conjugate composition and antigen concentration
  - Formulation
  - Antibody levels and IgG subclass analysis
  - RBD/Ace2 binding inhibition assay
  - Pseudoviral neutralization assay
- QUANTIFICATION AND STATISTICAL ANALYSIS

SUPPLEMENTAL INFORMATION

Supplemental information can be found online at https://doi.org/10.1016/j.isci.2022.104739.

ACKNOWLEDGMENTS

AUTHOR CONTRIBUTIONS

P.V.S. designed and coordinated experiments, analyzed data, and wrote the article. C.G.R & B.B.C synthesized and characterized conjugates, performed ELISA and isotyping assays. T.H.D. performed functional assays, provided reagents, and coordinated the pseudoviral neutralization studies, J.P.R provided antigen and reagents, L.E.L. supervised animal experiments E.K.B. & K.M.R prepared formulations, P.E.D. & N.H.T. obtained funding, coordinated the project, and edited the article. All authors participated in reviewing the article and have approved the final version.

DECLARATION OF INTERESTS

The authors declare that there are no competing interests.

REFERENCES

Alderson, J., Batchelor, V., O'Hanlon, M., Cifuentes, L., Richter, F.C., and Kopycinski, J.; Oxford-Cardiff COVID-19 Literature Consortium (2021). Overview of approved and upcoming vaccines for SARS-CoV-2: a living review. Oxf. Open Immunol. 2, iqab010. PMID: 34522886; PMCID: PMC8194545. https://doi.org/10.1093/oxfimm/iqab010.

Amanat, F., Stadlbauer, D., Strohmeier, S., Nguyen, T.H.O., Chromikova, V., McMahon, M., Jiang, K., Arunkumar, G.A., Jurczyszak, D., Polanco, J., et al. (2020). A serological assay to detect SARS-CoV-2 seroconversion in humans. Nat. Med. 26, 1033–1036. Epub 2020 May 12. PMID: 32398876; PMCID: PMC8183627. https://doi.org/10.1038/s41591-020-0913-5.

Armbruster, N., Jasny, E., and Petsch, B. (2019). Advances in RNA vaccines for preventive indications: a case study of A vaccine against rabies. Vaccines 7, 132. PMID: 31569785; PMCID: PMC6963972. https://doi.org/10.3390/vaccines7040132.

Baden, L.R., El Sahly, H.M., Essink, B., Kotloff, K., Frey, S., Novak, R., Diemert, D., Spector, S.A., Rouphael, N., Creech, C.B., et al. (2021). Efficacy and safety of the mRNA-1273 SARS-CoV-2 vaccine. N. Engl. J. Med. Overseas Ed. 384, 403–416. Epub 2020 Dec 30. PMID: 33378609; PMCID: PMC7787219. https://doi.org/10.1056/NEJMoa2035389.

Barda, N., Dagan, N., Cohen, C., Hernán, M.A., Lipsitch, M., Kohane, I.S., Reis, B.Y., and Balicer, R.D. (2021). Effectiveness of a third dose of the BNT162b2 mRNA COVID-19 vaccine for preventing severe outcomes in Israel: an observational study. Lancet 398, 2093–2100. Epub 2021 Oct 29. PMID: 34756184; PMCID: PMC8555967. https://doi.org/10.1016/S0140-6736(21)02249-2.

Bok, K., Sitar, S., Graham, B.S., and Mascola, J.R. (2021). Accelerated COVID-19 vaccine development: milestones, lessons, and prospects. Immunity 54, 1636–1651. Epub 2021 Aug 3. PMID: 34348117; PMCID: PMC8328682. https://doi.org/10.1016/j.immuni.2021.07.017.

Coccia, M., Collignon, C., Hervé, C., Chalon, A., Welsby, I., Detienne, S., van Helden, M.J., Dutta, S., Genito, C.J., Waters, N.C., et al. (2017). Cellular and molecular synergy in AS01-adjuvanted vaccines results in an early IFNγ response promoting vaccine immunogenicity. NPJ Vaccines 2, 25. Erratum in: NPJ Vaccines. 2018 Mar 21;3:13. PMID: 29263880; PMCID: PMC5627273. https://doi.org/10.1038/s41541-017-0027-3.

Collignon, C., Bol, V., Chalon, A., Surendran, N., Morel, S., van den Berg, R.A., Capone, S., Bechtold, V., and Temmerman, S.T. (2020). Innate immune responses to chimpanzee adenovirus

vector 155 vaccination in mice and monkeys. Front. Immunol. 11, 579872. PMID: 33329551; PMCID: PMC7734297. https://doi.org/10.3389/fimmu.2020.579872.

Corbett, K.S., Edwards, D.K., Leist, S.R., Abiona, O.M., Boyoglu-Barnum, S., Gillespie, R.A., Himansu, S., Schäfer, A., Ziwawo, C.T., DiPiazza, A.T., et al. (2020). SARS-CoV-2 mRNA vaccine design enabled by prototype pathogen preparedness. Nature 586, 567–571. Epub 2020 Aug 5. PMID: 32756549; PMCID: PMC7581537. https://doi.org/10.1038/s41586-020-2622-0.

Dickey, T.H., Tang, W.K., Butler, B., Ouahes, T., Orr-Gonzalez, S., Salinas, N.D., Lambert, L.E., and Tolia, N.H. (2021). Design of the SARS-CoV-2 RBD vaccine antigen improves neutralizing antibody response. Preprint at. bioRxiv. PMID: 34013270; PMCID: PMC8132226. https://doi.org/10.1101/2021.05.09.443238.

Du, L., He, Y., Zhou, Y., Liu, S., Zheng, B.J., and Jiang, S. (2009). The spike protein of SARS-CoV–a target for vaccine and therapeutic development. Nat. Rev. Microbiol. 7, 226–236. Epub 2009 Feb 9. PMID: 19198616; PMCID: PMC2750777. https://doi.org/10.1038/nrmicro2090.

Garçon, N., and Di Pasquale, A. (2017). From discovery to licensure, the Adjuvant System story. Hum. Vaccines Immunother. 13, 19–33. Epub 2016 Sep 16. PMID: 27636098; PMCID: PMC5287309. https://doi.org/10.1080/21645515.2016.1225635.

Gaspar, E.B., Prudencio, C.R., and De Gaspari, E. (2021). Experimental studies using OMV in a new platform of SARS-CoV-2 vaccines. Hum. Vaccines Immunother. 17, 2965–2968. Epub 2021 May 5. PMID: 33950776; PMCID: PMC8108191. https://doi.org/10.1080/21645515.2021.1920272.

Geng, Q., Tai, W., Baxter, V.K., Shi, J., Wan, Y., Zhang, X., Montgomery, S.A., Taft-Benz, S.A., Anderson, E.J., Knight, A.C., et al. (2021). Novel virus-like nanoparticle vaccine effectively protects animal model from SARS-CoV-2 infection. PLoS Pathog. 17, e1009897. PMID: 34492082; PMCID: PMC8448314. https://doi.org/10.1371/journal.ppat.1009897.

Hasegawa, H. (2021). Development of coronavirus-disease-19 vaccines. JMA J. 4, 187–190. Epub 2021 Jul 9. PMID: 34414311; PMCID: PMC8355660. https://doi.org/10.31662/jmaj.2021-0068.

Healy, S.A., Anderson, C., Swihart, B.J., Mwakingwe, A., Gabriel, E.E., Decederfelt, H., Hobbs, C.V., Rausch, K.M., Zhu, D., Muratova, O., et al. (2021). Pfs230 yields higher malaria transmission-blocking vaccine activity than Pfs25 in humans but not mice. J. Clin. Invest. 131,

e146221. PMID: 33561016; PMCID: PMC8011888. https://doi.org/10.1172/JCI146221.

Heath, P.T., Galiza, E.P., Baxter, D.N., Boffito, M., Browne, D., Burns, F., Chadwick, D.R., Clark, R., Cosgrove, C., Galloway, J., et al. (2021). Safety and efficacy of NVX-CoV2373 covid-19 vaccine. N. Engl. J. Med. 385, 1172–1183. Epub 2021 Jun 30. PMID: 34192426; PMCID: PMC8262625. https://doi.org/10.1056/NEJMoa2107659.

Hickey, J.M., Toprani, V.M., Kaur, K., Mishra, R.P.N., Goel, A., Oganesyan, N., Lees, A., Sitrin, R., Joshi, S.B., and Volkin, D.B. (2018). Analytical comparability assessments of 5 recombinant CRM197 proteins from different manufacturers and expression systems. J. Pharm. Sci. 107, 1806–1819. Epub 2018 Mar 8. PMID: 29526446. https://doi.org/10.1016/j.xphs.2018.03.002.

Hotez, P.J., and Bottazzi, M.E. (2022). Whole inactivated virus and protein-based COVID-19 vaccines. Annu. Rev. Med. 73, 55–64. Epub 2021 Oct 12. PMID: 34637324. https://doi.org/10.1146/annurev-med-042420-113212.

Hsieh, C.L., Goldsmith, J.A., Schaub, J.M., DiVenere, A.M., Kuo, H.C., Javanmardi, K., Le, K.C., Wrapp, D., Lee, A.G., Liu, Y., et al. (2020). Structure-based design of prefusion-stabilized SARS-CoV-2 spikes. Science 369, 1501–1505. Epub 2020 Jul 23. PMID: 32703906; PMCID: PMC7402631. https://doi.org/10.1126/science.abd0826.

Jackson, C.B., Farzan, M., Chen, B., and Choe, H. (2022). Mechanisms of SARS-CoV-2 entry into cells. Nat. Rev. Mol. Cell Biol. 23, 3–20. Epub 2021 Oct 5. PMID: 34611326; PMCID: PMC8491763. https://doi.org/10.1038/s41580-021-00418-x.

Jones, D.S., Rowe, C.G., Chen, B., Reiter, K., Rausch, K.M., Narum, D.L., Wu, Y., and Duffy, P.E. (2016). A method for producing protein nanoparticles with applications in vaccines. PLoS One 11, e0138761. PMID: 26950441; PMCID: PMC4780713. https://doi.org/10.1371/journal.pone.0138761.

Kirchdoerfer, R.N., Cottrell, C.A., Wang, N., Pallesen, J., Yassine, H.M., Turner, H.L., Corbett, K.S., Graham, B.S., McLellan, J.S., and Ward, A.B. (2016). Pre-fusion structure of a human coronavirus spike protein. Nature 531, 118–121. PMID: 26935699; PMCID: PMC4860016. https://doi.org/10.1038/nature17200.

Kleanthous, H., Silverman, J.M., Makar, K.W., Yoon, I.K., Jackson, N., and Vaughn, D.W. (2021). Scientific rationale for developing potent RBD-based vaccines targeting COVID-19. NPJ Vaccines 6, 128. PMID: 34711846; PMCID: PMC8553742. https://doi.org/10.1038/s41541-021-00393-6.

Lee, S., and Nguyen, M.T. (2015). Recent advances of vaccine adjuvants for infectious diseases. Immune Netw. 15, 51–57. Epub 2015 Apr 23. PMID: 25922593; PMCID: PMC4411509. https://doi.org/10.4110/in.2015.15.2.51.

Maharjan, P.M., and Choe, S. (2021). Plant-based COVID-19 vaccines: current status, design, and development strategies of candidate vaccines. Vaccines 9, 992. PMID: 34579229; PMCID: PMC8473425. https://doi.org/10.3390/vaccines9090992.

Martin, J.E., Louder, M.K., Holman, L.A., Gordon, I.J., Enama, M.E., Larkin, B.D., Andrews, C.A., Vogel, L., Koup, R.A., Roederer, M., et al. (2008). A SARS DNA vaccine induces neutralizing antibody and cellular immune responses in healthy adults in a Phase I clinical trial. Vaccine 26, 6338–6343. Epub 2008 Sep 26. PMID: 18824060; PMCID: PMC2612543. https://doi.org/10.1016/j.vaccine.2008.09.026.

Mendonça, S.A., Lorincz, R., Boucher, P., and Curiel, D.T. (2021). Adenoviral vector vaccine platforms in the SARS-CoV-2 pandemic. NPJ Vaccines 6, 97. PMID: 34354082; PMCID: PMC8342436. https://doi.org/10.1038/s41541-021-00356-x.

Nanishi, E., Borriello, F., O'Meara, T.R., McGrath, M.E., Saito, Y., Haupt, R.E., Seo, H.S., van Haren, S.D., Brook, B., Chen, J., et al. (2021). Alum:CpG adjuvant enables SARS-CoV-2 RBD-induced protection in aged mice and synergistic activation of human elder type 1 immunity. Preprint at. bioRxiv. PMID: 34031655; PMCID: PMC8142652. https://doi.org/10.1101/2021.05.20.444848.

Nanishi, E., Dowling, D.J., and Levy, O. (2020). Toward precision adjuvants: optimizing science and safety. Curr. Opin. Pediatr. 32, 125–138. PMID: 31904601; PMCID: PMC6970548. https://doi.org/10.1097/MOP.0000000000000868.

Natarajan, H., Crowley, A.R., Butler, S.E., Xu, S., Weiner, J.A., Bloch, E.M., Littlefield, K., Wieland-Alter, W., Connor, R.I., Wright, P.F., et al. (2020). SARS-CoV-2 antibody signatures robustly predict diverse antiviral functions relevant for convalescent plasma therapy. Preprint at. medRxiv. PMID: 32995801; PMCID: PMC7523138. https://doi.org/10.1101/2020.09.16.20196154.

Ndwandwe, D., and Wiysonge, C.S. (2021). COVID-19 vaccines. Curr. Opin. Immunol. 71, 111–116. Epub 2021 Jul 12. PMID: 34330017; PMCID: PMC8272971. https://doi.org/10.1016/j.coi.2021.07.003.

Nguyen, B., and Tolia, N.H. (2021). Protein-based antigen presentation platforms for nanoparticle vaccines. NPJ Vaccines 6, 70. PMID: 33986287; PMCID: PMC8119681. https://doi.org/10.1038/s41541-021-00330-7.

Pace, C.N., Vajdos, F., Fee, L., Grimsley, G., and Gray, T. (1995). How to measure and predict the molar absorption coefficient of a protein. Protein Sci. 4, 2411–2423. PMID: 8563639; PMCID: PMC2143013. https://doi.org/10.1002/pro.5560041120.

Pallesen, J., Wang, N., Corbett, K.S., Wrapp, D., Kirchdoerfer, R.N., Turner, H.L., Cottrell, C.A., Becker, M.M., Wang, L., Shi, W., et al. (2017). Immunogenicity and structures of a rationally designed prefusion MERS-CoV spike antigen. Proc. Natl. Acad. Sci. USA 114, E7348–E7357.

Epub 2017 Aug 14. PMID: 28807998; PMCID: PMC5584442. https://doi.org/10.1073/pnas.1707304114.

Pardi, N., Hogan, M.J., and Weissman, D. (2020). Recent advances in mRNA vaccine technology. Curr. Opin. Immunol. 65, 14–20. Epub 2020 Mar 31. PMID: 32244193. https://doi.org/10.1016/j.coi.2020.01.008.

Petsch, B., Schnee, M., Vogel, A.B., Lange, E., Hoffmann, B., Voss, D., Schlake, T., Thess, A., Kallen, K.J., Stitz, L., and Kramps, T. (2012). Protective efficacy of in vitro synthesized, specific mRNA vaccines against influenza A virus infection. Nat. Biotechnol. 30, 1210–1216. Epub 2012 Nov 25. PMID: 23159882. https://doi.org/10.1038/nbt.2436.

Pichichero, M.E. (2013). Protein carriers of conjugate vaccines: characteristics, development, and clinical trials. Hum. Vaccines Immunother. 9, 2505–2523. Epub 2013 Aug 16. PMID: 23955057; PMCID: PMC4162048. https://doi.org/10.4161/hv.26109.

Polack, F.P., Thomas, S.J., Kitchin, N., Absalon, J., Gurtman, A., Lockhart, S., Perez, J.L., Pérez Marc, G., Moreira, E.D., Zerbini, C., et al. (2020). Safety and efficacy of the BNT162b2 mRNA covid-19 vaccine. N. Engl. J. Med. 383, 2603–2615. Epub 2020 Dec 10. PMID: 33301246; PMCID: PMC7745181. https://doi.org/10.1056/NEJMoa2034577.

Richner, J.M., Himansu, S., Dowd, K.A., Butler, S.L., Salazar, V., Fox, J.M., Julander, J.G., Tang, W.W., Shresta, S., Pierson, T.C., et al. (2017). Modified mRNA vaccines protect against zika virus infection. Cell 168, 1114–1125.e10. PMID: 28222903; PMCID: PMC5388441. https://doi.org/10.1016/j.cell.2017.02.017.

Riener, C.K., Kada, G., and Gruber, H.J. (2002). Quick measurement of protein sulfhydryls with Ellman's reagent and with 4, 4'-dithiodipyridine. Anal. Bioanal. Chem. 373, 266–276. Epub 2002 Jun 6. PMID: 12110978. https://doi.org/10.1007/s00216-002-1347-2.

Sadoff, J., Gray, G., Vandebosch, A., Cárdenas, V., Shukarev, G., Grinsztejn, B., Goepfert, P.A., Truyers, C., Fennema, H., Spiessens, B., et al. (2021). Safety and efficacy of single-dose Ad26.COV2.S vaccine against covid-19. N. Engl. J. Med. 384, 2187–2201. Epub 2021 Apr 21. PMID: 33882225; PMCID: PMC8220996. https://doi.org/10.1056/NEJMoa2101544.

Sagara, I., Healy, S.A., Assadou, M.H., Gabriel, E.E., Kone, M., Sissoko, K., Tembine, I., Guindo, M.A., Doucoure, M., and Niaré, K., et al. (2018). Safety and immunogenicity of Pfs25H-EPA/Alhydrogel, a transmission-blocking vaccine against Plasmodium falciparum: a randomised, double-blind, comparator-controlled, dose-escalation study in healthy Malian adults. Lancet Infect. Dis. 18, 969–982. Epub 2018 Jul 27. PMID: 30061051; PMCID: PMC6287938. https://doi.org/10.1016/S1473-3099(18)30344-X.

Saunders, K.O., Lee, E., Parks, R., Martinez, D.R., Li, D., Chen, H., Edwards, R.J., Gobeil, S., Barr, M., Mansouri, K., et al. (2021). Neutralizing antibody vaccine for pandemic and pre-emergent coronaviruses. Nature 594, 553–559. Epub 2021 May 10. PMID: 33971664; PMCID: PMC8528238. https://doi.org/10.1038/s41586-021-03594-0.

Scaria, P.V., Anderson, C., Muratova, O., Alani, N., Trinh, H.V., Nadakal, S.T., Zaidi, I., Lambert, L., Beck, Z., Barnafo, E.K., et al. (2021). Malaria transmission-blocking conjugate vaccine in ALFQ adjuvant induces durable functional immune responses in rhesus macaques. NPJ Vaccines 6, 148. PMID: 34887448; PMCID: PMC8660773. https://doi.org/10.1038/s41541-021-00407-3.

Scaria, P.V., Chen, B., Rowe, C.G., Jones, D.S., Barnafo, E., Fischer, E.R., Anderson, C., MacDonald, N.J., Lambert, L., Rausch, K.M., et al. (2017). Protein-protein conjugate nanoparticles for malaria antigen delivery and enhanced immunogenicity. PLoS One 12, e0190312. PMID: 29281708; PMCID: PMC5744994. https://doi.org/10.1371/journal.pone.0190312.

Scaria, P.V., Chen, B.B., Rowe, C.G., Alani, N., Muratova, O.V., Barnafo, E.K., Lambert, L.E., Zaidi, I.U., Lees, A., Rausch, K.M., et al. (2020). Comparison of carrier proteins to conjugate malaria transmission blocking vaccine antigens, Pfs25 and Pfs230. Vaccine 38, 5480–5489. Epub 2020 Jun 26. PMID: 32600913. https://doi.org/10.1016/j.vaccine.2020.06.018.

Scaria, P.V., Rowe, C.G., Chen, B.B., Muratova, O.V., Fischer, E.R., Barnafo, E.K., Anderson, C.F., Zaidi, I.U., Lambert, L.E., Lucas, B.J., et al. (2019). Outer membrane protein complex as a carrier for malaria transmission blocking antigen Pfs230. NPJ Vaccines 4, 24. PMID: 31312527; PMCID: PMC6614402. https://doi.org/10.1038/s41541-019-0121-9.

Sebastian, M., Schröder, A., Scheel, B., Hong, H.S., Muth, A., von Boehmer, L., Zippelius, A., Mayer, F., Reck, M., Atanackovic, D., et al. (2019). A phase I/IIa study of the mRNA-based cancer immunotherapy CV9201 in patients with stage IIIB/IV non-small cell lung cancer. Cancer Immunol. Immunother. 68, 799–812. Epub 2019 Feb 15. PMID: 30770959. https://doi.org/10.1007/s00262-019-02315-x.

Shimp, R.L., Jr., Rowe, C., Reiter, K., Chen, B., Nguyen, V., Aebig, J., Rausch, K.M., Kumar, K., Wu, Y., Jin, A.J., et al. (2013). Development of a Pfs25-EPA malaria transmission blocking vaccine as a chemically conjugated nanoparticle. Vaccine 31, 2954–2962. Epub 2013 Apr 24. PMID: 23623858; PMCID: PMC3683851. https://doi.org/10.1016/j.vaccine.2013.04.034.

Shuler, K.R., Dunham, R.G., and Kanda, P. (1992). A simplified method for determination of peptide-protein molar ratios using amino acid analysis. J. Immunol. Methods 156, 137–149. PMID: 1474251. https://doi.org/10.1016/0022-1759(92)90020-t.

Stadlbauer, D., Amanat, F., Chromikova, V., Jiang, K., Strohmeier, S., Arunkumar, G.A., Tan, J., Bhavsar, D., Capuano, C., Kirkpatrick, E., et al. (2020). SARS-CoV-2 seroconversion in humans: a detailed protocol for a serological assay, antigen production, and test setup. Curr. Protoc. Microbiol. 57, e100. PMID: 32302069; PMCID: PMC7235504. https://doi.org/10.1002/cpmc.100.

Talaat, K.R., Ellis, R.D., Hurd, J., Hentrich, A., Gabriel, E., Hynes, N.A., Rausch, K.M., Zhu, D., Muratova, O., Herrera, R., et al. (2016). Safety and immunogenicity of pfs25-EPA/alhydrogel®, a transmission blocking vaccine against plasmodium falciparum: an open label study in malaria naïve adults. PLoS One 11, e0163144.

PMID: 27749907; PMCID: PMC5066979. https://doi.org/10.1371/journal.pone.0163144.

Tan, T.K., Rijal, P., Rahikainen, R., Keeble, A.H., Schimanski, L., Hussain, S., Harvey, R., Hayes, J.W.P., Edwards, J.C., McLean, R.K., et al. (2021). A COVID-19 vaccine candidate using SpyCatcher multimerization of the SARS-CoV-2 spike protein receptor-binding domain induces potent neutralising antibody responses. Nat. Commun. 12, 542. PMID: 33483491; PMCID: PMC7822889. https://doi.org/10.1038/s41467-020-20654-7.

Tao, K., Tzou, P.L., Nouhin, J., Gupta, R.K., de Oliveira, T., Kosakovsky Pond, S.L., Fera, D., and Shafer, R.W. (2021). The biological and clinical significance of emerging SARS-CoV-2 variants. Nat. Rev. Genet. 22, 757–773. Epub 2021 Sep 17. PMID: 34535792; PMCID: PMC8447121. https://doi.org/10.1038/s41576-021-00408-x.

Tay, M.Z., Wiehe, K., and Pollara, J. (2019). Antibody-dependent cellular phagocytosis in antiviral immune responses. Front. Immunol. 10, 332. PMID: 30873178; PMCID: PMC6404786. https://doi.org/10.3389/fimmu.2019.00332.

Tian, J.H., Patel, N., Haupt, R., Zhou, H., Weston, S., Hammond, H., Logue, J., Portnoff, A.D., Norton, J., Guebre-Xabier, M., et al. (2021). SARS-CoV-2 spike glycoprotein vaccine candidate NVX-CoV2373 immunogenicity in baboons and protection in mice. Nat. Commun. 12, 372. PMID: 33446655; PMCID: PMC7809486. https://doi.org/10.1038/s41467-020-20653-8.

Toledo-Romani, M.E., Garcia-Carmenate, M., Silva, C.V., Baldoquin-Rodriguez, W., Pérez, M.M., Gonzalez, M.C.R., Moreno, B.P., Hernández, I.C.M., Romero, R.G.-M., Tabio, O.S., et al. (2021). Efficacy and safety of SOBERANA 02, a COVID-19 conjugate vaccine in heterologous three-dose combination. Preprint at medRxiv. https://doi.org/10.1101/2021.10.31.21265703.

Valdes-Balbin, Y., Santana-Mederos, D., Quintero, L., Fernández, S., Rodriguez, L., Sanchez-Ramirez, B., Perez-Nicado, R., Acosta, C., Méndez, Y., Ricardo, M.G., et al. (2021). SARS-CoV-2 RBD-tetanus toxoid conjugate vaccine induces a strong neutralizing immunity in preclinical studies. ACS Chem. Biol. 16, 1223–1233. Epub 2021 Jul 4. PMID: 34219448. https://doi.org/10.1021/acschembio.1c00272.

Volpatti, L.R., Wallace, R.P., Cao, S., Raczy, M.M., Wang, R., Gray, L.T., Alpar, A.T., Briquez, P.S., Mitrousis, N., Marchell, T.M., et al. (2021). Polymersomes decorated with the SARS-CoV-2 spike protein receptor-binding domain elicit robust humoral and cellular immunity. ACS Cent. Sci. 7, 1368–1380. Epub 2021 Jul 21. PMID: 34466656; PMCID: PMC8315245. https://doi.org/10.1021/acscentsci.1c00596.

Voss, W.N., Hou, Y.J., Johnson, N.V., Delidakis, G., Kim, J.E., Javanmardi, K., Horton, A.P., Bartzoka, F., Paresi, C.J., Tanno, Y., et al. (2021). Prevalent, protective, and convergent IgG recognition of SARS-CoV-2 non-RBD spike epitopes. Science 372, 1108–1112. Epub 2021 May 4. PMID: 33947773; PMCID: PMC8224265. https://doi.org/10.1126/science.abg5268.

Voysey, M., Clemens, S.A.C., Madhi, S.A., Weckx, L.Y., Folegatti, P.M., Aley, P.K., Angus, B., Baillie, V.L., Barnabas, S.L., Bhorat, Q.E., et al. (2021). Safety and efficacy of the ChAdOx1 nCoV-19 vaccine (AZD1222) against SARS-CoV-2: an interim analysis of four randomised controlled trials in Brazil, South Africa, and the UK. Lancet 397, 99–111. PMID: 33306989; PMCID: PMC7723445. https://doi.org/10.1016/S0140-6736(20)32661-1.

Walls, A.C., Fiala, B., Schäfer, A., Wrenn, S., Pham, M.N., Murphy, M., Tse, L.V., Shehata, L., O'Connor, M.A., Chen, C., et al. (2020). Elicitation of potent neutralizing antibody responses by designed protein nanoparticle vaccines for SARS-CoV-2. Cell 183, 1367–1382.e17. Epub 2020 Oct 31. PMID: 33160446; PMCID: PMC7604136. https://doi.org/10.1016/j.cell.2020.10.043.

Wong, T.Y., Lee, K.S., Russ, B.P., Horspool, A.M., Kang, J., Winters, M.T., Wolf, A.M., Rader, N.A., Miller, O.A., Shiflett, M., et al. (2022). Intranasal administration of BReC-CoV-2 COVID-19 vaccine protects K18-hACE2 mice against lethal SARS-CoV-2 challenge. NPJ Vaccines 7, 36. PMID: 35288576; PMCID: PMC8921182. https://doi.org/10.1038/s41541-022-00451-7.

Xiaojie, S., Yu, L., Lei, Y., Guang, Y., and Min, Q. (2020). Neutralizing antibodies targeting SARS-CoV-2 spike protein. Stem Cell Res. 50, 102125. Epub ahead of print. PMID: 33341604; PMCID: PMC7737530. https://doi.org/10.1016/j.scr.2020.102125.

STAR★METHODS

KEY RESOURCES TABLE

REAGENT or RESOURCE	SOURCE	IDENTIFIER
Antibodies		
Peroxidase conjugated anti-mouse IgG	Jackson ImmunoResearch Laboratories	115-035-164; RRID:AB_2338510
Peroxidase conjugated human IgG	Jackson ImmunoResearch Laboratories	109-035-098; RRID:AB_2337586
Goat anti-mouse IgG1-AP conjugate	Southern Biotech	1071–04; RRID:AB_2794425
Goat anti-mouse IgG2a-AP conjugate	Southern Biotech	1083–04; RRID:AB_2794508
Goat anti-mouse IgG2b-AP conjugate	Southern Biotech	1091–04; RRID:AB_2794541
Goat anti-mouse IgG3-AP conjugate	Southern Biotech	1100–04; RRID:AB_2794572
Bacterial and virus strains		
SARS-CoV-2 Pseudovirus (WA)	GenScript	SC2087A
Biological samples		
Fetal Bovine Serum (FBS)	Gibco	10099–141C
Chemicals, peptides, and recombinant proteins		
ExpiFectamine	Thermo Fisher	A14524
Polyethyleneimine	Polyscience	23966–1
Fire-Lumi Luciferase assay system	GenScript	L00877C-1000
Tetramethylbenzidine	MilliporeSigma	T0440
Phosphatase substrate	Sigma-Aldrich	S0942
N-(ε-maleimidocaproyloxy- succinimide)	Pierce Biotechnology	22308
(N-succinimidyl S-acetylthioacetate) (SATA)	Pierce Biotechnology	26102
BupH PBS pack	Pierce Biotechnology	28372
Protein A agarose resin	GoldBio	P-400-5
Opti-MEM	Gibco	31985–070
DMEM Medium	Gibco	10569–010
Protein A IgG binding buffer	Thermo Fisher	21001
IgG elution buffer	Thermo Fisher	21004
Critical commercial assays		
AAA analysis	Dana Farber Cancer Institute	https://www.dana-farber.org/research/core-facilities/
Pseudovirus neutralization assay	GenScript	https://www.genscript.com/
Experimental models: Cell lines		
Expi293	Thermo Fisher	A14527
ACE2 overexpressing cells	GenScript	RD00825
Experimental models: Organisms/strains		
CD-1 mice	Charles River	https://www.criver.com/products-services/find-model/cd-1r-igs-mouse?region=3611
Recombinant DNA		
ACE2-Fc fusion plasmid	Addgene	145163

Continued

REAGENT or RESOURCE	SOURCE	IDENTIFIER
Software and algorithms		
Prism	GraphPad Software Inc., La Jolla, CA	https://www.graphpad.com/
Other		
Alhydrogel®	CRODA, Denmark	5594
AS01	Glaxo Smith Kline	SHINGRIX Kit- ZH5R5
HPLC-SEC	Agilent	Agilent 1200 HPLC System
SEC-MALS detectors - Wyatt DAWN GELIOS II	Wyatt Technologies, Santa Barbara, CA	S/N 881-H2
SEC-MALS detectors - OptiLab TrEX	Wyatt Technologies, Santa Barbara, CA	Serial #: 1282-TREX
AKTA Pure FPLC	Cytiva	ÄKTA pure 25 L
NanoDrop One Spectrophotometer	Thermo Fisher	ND2000USCAN
S41i-CO2 incubator shaker	Eppendorf	S41I120010
Hiload 16/60 Superdex column	Pharmacia Biotech	Code number:17-1069-01 Id number: 0636006
TSKgel G5000PWxl column	Tosoh Bioscience	Cat: 08023 Column #: N0020-12k
HisTrap Excel NTA column	Cytiva	17371206
Superdex 200 GL column	Cytiva	28990944
Microplate reader	BMG	PHERAStar FSX
Centrifuge	Beckman Coulter	AllegraX-15R
Inverted microscope	DIANYING	37XC
Cell incubator	Thermo Scientific	Forma Series II
CFD10 10 kDa cutoff	Millipore, Billerica, MA	Ref #: UFC901096 Lot: R8EA70722
CFD100, 100 kDa cutoff	Millipore, Billerica, MA	Ref#: UFC910024 Lot: R3KA73079
ELISA plates – Nunc MaxiSorp	Thermo Fisher	44-2404-21

RESOURCE AVAILABILITY

Lead contact

Further information and requests for resources and reagents should be directed to and will be fulfilled by the lead contact, Patrick E. Duffy (patrick.duffy@nih.gov).

Materials availability

This study did not generate new unique reagents.

Data and code availability

- All data reported in this paper will be shared by the lead contact upon request.
- This paper does not report original code.
- Any additional information required to reanalyze the data reported in this paper is available from the lead contact upon request.

EXPERIMENTAL MODEL AND SUBJECT DETAILS

Mouse immunogenicity study

Immunogenicity of various conjugates and unconjugated antigen were evaluated in 5 to 6 weeks old, healthy female CD-1 mice (obtained from Charles River Laboratories, Wilmington, MA). Animal studies

were performed in an AAALAC-accredited facility in accordance with an animal study protocol guided and approved by the Institutional Animal Care and Use Committee (IACUC) at the National Institutes of Health. Animals were housed in SPF-filtered micro-isolators; nestlets were used for enrichment with food and water administered *ad libitum*.

10 mice per group were used for each test sample. Mice were vaccinated by intra-muscular injection of 50 μL Alhydrogel® or AS01 formulations on Days 0 and 21. Blood samples from animals were collected by cardiac puncture, after anesthesia on days 14 and 35. Sera obtained were analyzed for anti-RBD antibody titer by ELISA and functional activity by pseudovirus neutralization assay, described below.

METHOD DETAILS

Expression of full-length spike protein and receptor binding domain of SARS-CoV-2

Plasmids expressing the Receptor Binding Domain (RBD) and full-length spike proteins were generous gifts of Florian Krammer, Icahn School of Medicine at Mount Sinai. Production of these proteins was performed in a similar manner to previous methods (Stadlbauer et al., 2020; Amanat et al., 2020). Typically, Expi293 (Thermo Fisher) suspension cells in 293F Expi293 Expression medium (Thermo Fisher) were grown at 37°C and 8% CO_2, maintaining cultures at continuous log phase growth ($3.0–5x10^6$) for 3-4 passages after thawing. The day before transfection, 500 mL of culture was seeded at a density of $2.5–3x10^6$ cells/mL in a 2 L flask. The day of transfection, cells were diluted back to $2.5–3x10^6$ prior to transfection. Expi293 cells were transfected using 1.4 mL of ExpiFectamine™ (Thermo Fisher) and 0.5 mg of plasmid DNA per 0.5 L of cells. Plasmid DNA was diluted into 25 mL of OptiMEM (Thermo Fisher) and filter sterilized through a 0.2 micron filter. The ExpiFectamine™ was slowly added to 25 mL of OptiMEM, gently mixed and incubated for 5 min. The diluted ExpiFectamine™ was then added slowly to the diluted DNA, gently mixed and incubated at room temperature for 10–20 min. The mixture was added to the cells slowly while swirling the flask. The flask was returned to the incubator at 37°C and 8% CO_2 for 16–20 h. The following day, both enhancer I and II (Thermo Fisher) were added to the Expi293 cultures and returned to the incubator. Cultures at 4 days post-transfection were centrifuged at 10,000 × g for 30 min. The spent culture media was sequentially filtered through 0.45 μm and 0.2 μm filters. The clarified spent media was loaded on a 5 mL HisTrap™ Excel NTA column (GE Life Sciences). The column was washed with 20 column volumes of wash buffer (20 mM sodium phosphate, 0.5 M NaCl, 0 to 30 mM imidazole, pH 7.4). The bound protein was eluted with a step gradient of elution buffer (20 mM sodium phosphate, 0.5 M NaCl, 500 mM imidazole, pH 7.4). The eluted NTA fractions were confirmed to contain RBD or full-length spike proteins by SDS-PAGE (4–12% Bis-tris, Thermo Fisher) and Coomassie staining. The fractions were pooled, concentrated, and buffer exchanged by diafiltration using a 10 kDa cutoff centrifugal filter unit (Millipore Sigma). The absorbance at 280 nm was determined and the concentration of the recombinant spike or RBD was calculated from the predicted extinction coefficient from the protein sequence. Proteins were then aliquoted and stored at −80°C.

Ace2-Fc expression and purification

The Ace2-Fc fusion was expressed from pcDNA3: pcDNA3-sACE2(WT)-Fc(IgG1) was a gift from Erik Procko (Addgene plasmid # 145163; http://n2t.net/addgene:145163; RRID:Addgene_145163). Expi293F cells were transfected with the plasmid according to manufacturer's instructions and supernatant was harvested after 4 days of expression (Thermo Fisher Scientific). Supernatant was incubated with protein A agarose resin at room temperature (GoldBio) for 1 h. Resin was collected and washed with 10 column volumes protein A IgG binding buffer (Thermo Fisher Scientific). Protein was then eluted with 10 column volumes of IgG elution buffer (Thermo Fisher Scientific) and neutralized with 1 column volume of 1 M Tris pH 9.0. Ace2-Fc was further purified by size-exclusion chromatography using a Superdex 200 Increase 10/300 GL column (Cytiva) equilibrated in 1× PBS.

Recombinant protein carrier, EcoCRM® with a molecular weight of 58,412.6 Da, produced in *E. coli* with an oxidative intracellular environment, were obtained from Fina Biosolutions, Rockville, MD (Hickey et al., 2018).

Adjuvants

Alhydrogel® 2% (9–11 mg/mL of Al) was purchased from CRODA, Denmark. AS01 containing the TLR4 agonist MPL (100 ug/mL) and saponin fraction QS-21 (100 ug/mL) in a liposomal formulation was obtained

from commercially available SHINGRIX vaccine package. A final delivery dose in mice contained 2.5 μg/ 2.5 μg (MPL/QS-21) per 0.05 mL dose.

Chemicals and reagents

N-(ε-maleimidocaproyloxy-succinimide) (EMCS) and (N-succinimidyl S-acetylthioacetate) (SATA) were from Pierce Biotechnology Inc. (Rockford, IL). All buffers were prepared from BupH PBS Pack. Deacetylation buffer containing 0.5M NH_2OH was prepared with pH 7.2 PBSE. Amicon centrifugal filtration devices CFD10 and CFD100 with 10 kDa and 100 kDa MWCO respectively were obtained from Millipore (Billerica, MA).

Maleimide modified EcoCRM

A solution of 7.84 mg of EcoCRM in 3.6 mL of pH 7.2 PBSE (100 mM sodium phosphate, 150 mM NaCl, 5 mM EDTA) (2.178 mg/mL, 1.34×10^{-7} mol) was equilibrated in a 22°C water bath with stirring. To this solution 40.3 μL of a 30.8 mg/mL solution of EMCS in DMSO (1.24 mg, 4.03×10^{-6} mol) was added and the mixture was stirred for 1.5 h at 22°C. The buffer of the mixture was exchanged with pH 6.5 phosphate buffered sucrose (10 mm sodium phosphate, 10% sucrose) (1000-fold exchange) using a CFD10 to obtain 1.7 mL of maleimide modified EcoCRM. An indirect DTDP assay determined the number of maleimides per molecule of EcoCRM to be 7.68. The protein concentration was determined to be 4.77 mg/mL.

Sulfhydryl modified RBD

To a solution of 2.43 mg (9.68×10^{-8} mol) of RBD in 1.2 mL of pH 7.2 PBSE buffer (100 mM sodium phosphate, 150 mM NaCl, 5 mM EDTA), stirred at 22°C, 19.4 μL (0.447 mg, 1.94×10^{-6} mol) of a 23 mg/mL solution of SATA linker in DMSO was added and stirred for 1 h at 22°C. The mixture was diluted with pH 7.2 PBSE (100 mM sodium phosphate, 150 mM NaCl, 5 mM EDTA) and concentrated repeatedly to affect a 1000-fold buffer exchange using a CFD10 to give a final volume of approximately 1.0 mL (2 mg/mL). To the resulting solution (1.0 mL) was added 0.10 mL of deacetylation buffer (0.5 M NH_2OH in pH 7.2 PBSE). The mixture was placed on a rotating shaker at 600 RPM for 1 h at 22°C. The mixture was transferred to a CFD10, and the buffer was exchanged into pH 6.5 PBSE (100 mM sodium phosphate, 150 mM NaCl, 5 mM EDTA) by repeated dilution and concentration to affect a 1000-fold buffer exchange, yielding 1.4 mL of a 1.49 mg/mL solution of sulfhydryl modified RBD (2.08 mg). The product was kept frozen at −80°C until used. DTDP assay showed 2.73 thiols per molecule of RBD.

Synthesis of RBD-EcoCRM crosslinked conjugate (CC)

Crosslinked conjugate of RBD with EcoCRM, (RBD-EcoCRM-CC) was synthesized as described below using the procedure described previously for Pfs230-EcoCRM conjugate (Scaria et al., 2020).

To 0.30 mL of a 4.77 mg/mL solution of maleimide modified EcoCRM in pH 6.5 phosphate buffered sucrose (1.45 mg, 2.48×10^{-8} moles), with stirring in a 22°C water bath, 1.73 mL of pH 6.5 PBSE was added. This was followed by addition of 1.2 mL of a 1.49 mg/mL solution of sulfhydryl modified RBD (1.788 mg, 7.12×10^{-8} mol) in pH 6.5 PBSE, and the mixture was stirred for 1 h at 22°C. The excess maleimide groups were quenched by adding 42 μL of a 0.8 mg/mL solution of cysteine hydrochloride (0.034 mg, 1.91×10^{-7} mol) in pH 6.5 PBSE, and the mixture was stirred an additional 15 min. Purification was carried out by gel filtration chromatography using a a HiLoad™ 16/60 Superdex 200 prep grade column at 30 mL/h flow rate in PBS. One mL fractions were collected across the protein peak and were analyzed by size exclusion chromatography (G5000PWxl column). Fractions eluting from 56–76 min were combined to give 1.095 mg of product at a concentration of 0.996 mg/mL, as determined by absorbance at 280 nm. Molecular weight and distribution were determined by SEC MALS analysis which gave an average molecular weight of 1,364 kDa (Table 1B).

Synthesis of RBD-EcoCRM radial conjugate (RC)

To a 1.75 mL solution of 3.06 mg (1.22×10^{-7} mol) of RBD in PBS was added 5 molar equivalents of DTT (4.71 μL of a 20 mg/mL solution of DTT in 100 mM Acetate Buffered Saline pH 4.5). The mixture was vortexed and placed on an orbital shaker at 600 RPM at room temperature for 30 min. The mixture was diluted with 100 mM PBS +5mM EDTA pH6.5 (PBSE_6.5) and concentrated repeatedly to affect a 120-fold buffer exchange using a Millipore centrifugal filtration device (10 kDa MWCO) to give a final volume of

1.10 mL. The final protein concentration was determined to be 2.72 mg/mL of RBD-SH by A280. A Direct DTDP assay determined the number of thiols per RBD-SH was 1.2.

180.6 μL of a 4.77 mg/mL solution of maleimide-activated EcoCRM (0.861 mg, 1.47×10^{-8} mol EcoCRM) in PBSE_6.5, containing 7.7 maleimide groups per EcoCRM molecule, was diluted with 2,315 μL of PBSE_6.5. To this solution was added 950 μL of the 2.72 mg/mL solution of de-protected RBD-SH (2.58 mg, 1.03×10^{-7} mol) in PBSE_6.5. The mixture was vortexed and placed on an orbital shaker at 600 RPM for 30 min at room temperature. Excess maleimides were quenched by the addition of 19.9 μL of a 10 mg/mL solution of L-cysteine hydrochloride (0.199 mg, 1.13×10^{-6} mol) in PBSE_6.5 was added. After five minutes, the quenched conjugation was spun down for 2 min at 2k RCF to pellet any precipitates, and the supernatant was purified by fractionation on a HiLoad™ 16/60 Superdex 200 prep grade column at 30 cm/h in PBS. 1.0 mL fractions were collected across the protein peak as detected by absorbance at 280 nm. Fractions eluting from 70–85 min were pooled, concentrated using a Millipore centrifugal filtration device (100 kDa MWCO), and sterile-filtered (0.22-μm PVDF) to yield 640 μL of RBD-EcoCRM-RC in PBS.

Determination of thiol and maleimide modifications

Average number of free thiol groups in the antigen and maleimide modifications on EcoCRM were assayed as described previously (Scaria et al., 2020). Number of thiol moieties in the sulfhydryl modified RBD were determined by 4,4′-dithiodipyridine (DTDP) assay. Sulfhydryl modified antigens were reacted with DTDP at pH 6.5 and the concentration of released 4-thiopyridon was determined from the absorbance at 324 nm using a molar extinction coefficient of 21,400 L M^{-1} (Riener et al., 2002). The assay was validated by cysteine standards included in the assay. The number of maleimide moieties in the maleimide modified EcoCRM was determined by a "reverse-DTDP" assay. In this assay, the DTDP assay is used to determine the amount of cysteine consumed by maleimide moieties, when incubated with known amount of cysteine. Maleimide-modified proteins mixed with standard cysteine solutions were incubated for 1 h at room temperature. Thiol concentration of the mixtures were then measured by DTDP assay. Maleimide concentration was calculated as the difference between the thiol concentration of the standard cysteine solution and the cysteine plus maleimide-modified protein.

Determination of conjugate molecular weight

The weighted-average molecular weight and molecular weight distributions of RBD conjugates were determined by SEC-MALS detectors (Wyatt DAWN HELIOS II and OptiLab TrEX, Wyatt Technologies, Santa Barbara, CA) using ASTRA 7.3 software, as previously described (Scaria et al., 2020). Average molar weight (Mw) and molecular weight distribution of the conjugates were determined using ASTRA software.

Determination of conjugate composition and antigen concentration

Composition of RBD-EcoCRM conjugates (antigen-to-carrier ratio) was determined from amino acid analyses of the conjugates and individual protein components (antigen and carrier) using a method previously described (Scaria et al., 2020). The molar ratios of the proteins in the conjugates were calculated by a multiple regression analysis of the amino acid analysis data with least square fitting, using a selected set of amino acids common to both proteins (Shuler et al., 1992). Amino acid analyses were carried out at the Molecular Biology Core Facility at the Dana Farber Cancer Institute (MBCF-DFCI), Boston, Massachusetts. An extinction coefficient was derived from the antigen-to-carrier ratio using the theoretical extinction coefficients of both monomeric components (Pace et al., 1995) to determine the antigen concentration for both conjugates based on their A280 readings.

Formulation

Conjugates for mouse immunogenicity studies were formulated in either Alhydrogel® or in AS01, a liposomal adjuvant containing MPL and QS-21. Alhydrogel formulated immunogens contained 0.45 mg/mL Alhydrogel® (aluminum content) and were prepared within 24 h of vaccination and stored at 2-8°C until used. AS01 formulations were prepared within 4 h of vaccination by mixing an equal volume of the adjuvant with the conjugate solution to obtain a final concentration of 2.5 μg of MPL and 2.5 μg of QS-21 in 50 μL of injection volume.

Antibody levels and IgG subclass analysis

Anti-RBD antibody titers were assayed using standard ELISA method described previously,[10] with full length Spike protein as the plate antigen (Healy et al., 2021). Briefly, plates (Nunc MaxiSorp;

ThermoFisher Scientific) were coated with 100 μL 0.01 mg/mL purified trimeric FL-spike ectodomain diluted in 50 mM Na-carbonate pH 9.5 and incubated overnight at 4°C. Plates were washed three times with PBST, blocked with 2% BSA in PBST for 1 h at room temperature and washed again three times with PBST. Serum was diluted in 2% BSA in PBST and 100 μL was added to each well and incubated for 1 h incubation at room temperature. Plates were then washed three times with PBST and 200 μL each of 1:5000 peroxidase conjugated anti-mouse IgG was added (Jackson ImmunoResearch Laboratories, Inc. Cat. # 115- 035–164). After incubation for 30 min at room temperature, they were washed with PBST three times. 70 μL Tetramethylbenzidine (TMB) (MilliporeSigma) was added to the wells and incubated for 20 min at room temperature before quenching with 70 μL 2 M H2SO4. Absorbance at 450 nm was measured using a plate reader.

Pooled serum from mice immunized with RBD was used to generate a standard curve on each plate to calculate the antibody titers of individual animals in different groups. One antibody unit (AU) was defined as the dilution of the standard serum required to achieve an absorbance value of 1 at 450 nm. Each plate included triplicate 2-fold serial dilutions of the standard serum from 20 to 0.01 AU. Serum from each animal was diluted such that the absorbance at 450 nm fell in the informative region of the standard curve between 0.1 and 2.0. The absorbance values at 450 nm for the standard curve were fit to a 4-parameter logistic curve, which was used to convert absorbance values to AU for each individual animal. AU values for each individual animal were measured in triplicate on separate plates and the average is reported.

For IgG subclass analyses, sera from each group of mice were pooled and diluted 500-fold in Blocking Buffer. ELISA's were performed for each pooled group as per the method used to determine the anti-RBD titers, with the exception that the Goat-anti-Mouse secondary antibodies were IgG1-, IgG2a-, IgG2b-, or IgG3-specific Alkaline Phosphatase-conjugates (Southern Biotech), a Phosphatase substrate (Sigma, Cat. #S0942) was used as the developer, and the absorbance values were determined by subtracting the A650nm from the A405nm readings after developing for 20 min. Each IgG subclass (IgG1, IgG2a, IgG2b and IgG3) titer was determined and expressed as a % contribution to the sum of subclasses.

RBD/Ace2 binding inhibition assay

The RBD/Ace2 blocking assay was performed, as described previously (Dickey et al., 2021). Nunc MaxiSorp plates (ThermoFisher Scientific) were coated with 100 μL 0.32 μg/mL purified RBD diluted in 50 mM Na-carbonate pH 9.5. Plates were incubated overnight at 4°C followed by washing three times with PBST. Plates were then blocked for one hour at room temperature with 2% BSA in PBST and washed three times with PBST. Serum was diluted in 2% BSA in PBST in a 3-fold dilution series from 1:100 to 1:218,700. 50 μL serum was mixed with 10 μL 30 nM Ace2-Fc or 10 μL buffer as a background control. 50 μL serum mixture was added to RBD-coated plates and incubated 1 h at room temperature. Plates were washed three times with PBST and 200 μL 1:30,000 peroxidase-conjugated anti-human IgG was added (Jackson ImmunoResearch Laboratories, Inc. Cat. # 109-035-098). Plates were incubated 30 min at room temperature and washed three times with PBST. Finally, 70 μL Tetramethylbenzidine (TMB) (MilliporeSigma) was added to each well and incubated for 20 min at room temperature before quenching with 70 μL each of 2 M H_2SO_4. Absorbance at 450 nm was measured using a Biotek Synergy H1 plate reader.

RBD/Ace2 binding inhibition was calculated after subtracting the Abs_{450} values of the background controls lacking Ace2-Fc. Four wells without serum were used to calculate the maximum signal. Inhibition was calculated using the following formula:

$$\% \ inhibition \ = \ 100 \times \left(1 - \frac{X}{\max}\right)$$

where X is the Abs_{450} of a well after background-subtraction and max is the average of the four samples without serum after background-subtraction.

% inhibition values were fit using a normalized dose-response curve with a variable slope:

$$Y \ = \ 100 \left/ \left(1 + \left(\frac{IC50}{X}\right) \hat{} HillSlope\right)\right.$$

where X is the serum dilution, Y is the % inhibition, and HillSlope and IC_{50} are calculated parameters corresponding to the slope of the curve and the dilution at which 50% inhibition occurs, respectively. IC_{50} values for each animal were log-transformed and plotted, along with the geometric mean value for each group.

Pseudoviral neutralization assay

Serum mediated neutralization of viral entry into Ace2 expressing cells were assayed using a pseudovirus consisting of spike protein (WA-1) and expressing luciferase reporter gene as described previously (Dickey et al., 2021). Mouse serum was diluted in a triplicate 5-fold series from 1:10 to 1:781,250. Serum was mixed 1:1 with pseudovirus expressing luciferase reporter gene in a 96-well plate (GenScript). After incubation at room temperature for 1 h, 20,000 HEK293 cells overexpressing Ace2 were added to each well. Cells were incubated with pseudovirus at 37°C, 5% CO_2 for 48 h, after which culture medium was removed and Fire-Lumi^{TM} luciferase substrate reagent was added to the wells. Luciferase signal was measured using an PHERAStar microplate reader and %inhibition was calculated using the following formula:

$$\% \ inhibition \ = \ 100 \times \left(1 - \frac{X - min}{max - min} \right)$$

where X is the luciferase signal, min is the average signal from duplicate wells without pseudovirus, and max is the average signal from duplicate wells without serum. Log IC_{50} values were calculated in the same manner described for the RBD/Ace2 blocking assay.

QUANTIFICATION AND STATISTICAL ANALYSIS

Data were analyzed with Prism software (GraphPad Software, Inc., La Jolla, CA). Statistical differences between test groups ($p \leq 0.05$) were measured using a Kruskal-Wallis analysis followed by a Dunn multiple comparator test for comparing three or more groups.